



EUROPEAN ORGANIZATION FOR NUCLEAR RESEARCH

CERN-EP/90-23

19 February 1990

**SEARCH FOR DECAYS OF THE Z^0
INTO A PHOTON AND A PSEUDOSCALAR MESON**

The ALEPH Collaboration*)

ABSTRACT

A search is reported for decays of the Z^0 into $\pi^0\gamma$, $\eta\gamma$ and $\eta'(958)\gamma$ in e^+e^- collisions using data collected during a scan around the Z^0 mass. In order to search for $\pi^0\gamma$ final states, in which the two photons from the π^0 decay are unresolved, the production of pairs of high-energy electromagnetic clusters is studied. The data are compared with the expectations from the pure QED process $e^+e^- \rightarrow \gamma\gamma$, and a 95% confidence level upper limit on the branching ratio of the Z^0 into $\pi^0\gamma$ of 4.9×10^{-4} is derived. For $\eta'\gamma$, the decay modes of the mesons that contain two charged particles are largely free from QED background. These modes are used to place upper limits of 4.6×10^{-4} and 2.2×10^{-4} on the corresponding branching ratios of the Z^0 .

(Submitted to Physics Letters B)

*) See next pages for the list of authors

- D. Decamp, B. Deschizeaux, C. Goy, J.-P. Lees, M.-N. Minard
Laboratoire de Physique des Particules (LAPP), IN²P³-CNRS, 74019 Annecy-le-Vieux Cedex, France
- J.M. Crespo, M. Delfino, E. Fernandez¹, M. Martinez, R. Miquel, Ll.M. Mir, S. Orteu, A. Pacheco, J.A. Perlas, E. Tubau
Laboratorio de Fisica de Altas Energias, Universidad Autonoma de Barcelona, 08193 Bellaterra (Barcelona), Spain¹⁰
- M.G. Catanesi, M. de Palma, A. Farilla, G. Iaselli, G. Maggi, S. Natali, S. Nuzzo, A. Ranieri, G. Raso, F. Romano, F. Ruggieri, G. Selvaggi, L. Silvestris, P. Tempesta, G. Zito
INFN Sezione di Bari e Dipartimento di Fisica dell' Universita', 70126 Bari, Italy
- Y. Gao, H. Hu, D. Huang, S. Jin, J. Lin, T. Ruan, T. Wang, W. Wu, Y. Xie, D. Xu, R. Xu, J. Zhang, Z. Zhang, W. Zhao
Institute of High-Energy Physics, Academia Sinica, Beijing, The People's Republic of China¹¹
- H. Albrecht², W.B. Atwood³, F. Bird, E. Blucher, T.H. Burnett⁴, T. Charity, H. Drevermann, Ll. Garrido, C. Grab, R. Hagelberg, S. Haywood, B. Jost, M. Kasemann, G. Kellner, J. Knobloch, A. Lacourt, I. Lehraus, T. Lohse, D. Lüke², A. Marchioro, P. Mato, J. May, A. Minten, A. Miotto, P. Palazzi, M. Pepe-Altarelli, F. Ranjard, A. Roth, J. Rothberg⁴, H. Rotscheidt, W. von Rüden, R. St.Denis, D. Schlatter, M. Takashima, M. Talby⁵, H. Taureg, W. Tejessy, H. Wachsmuth, S. Wheeler, W. Wiedenmann, W. Witzeling, J. Wotschack
European Laboratory for Particle Physics (CERN), 1211 Geneva 23, Switzerland
- Z. Ajaltouni, M. Bardadin-Otwinowska, A. Falvard, P. Gay, P. Henrard, J. Jousset, B. Michel, J-C. Montret, D. Pallin, P. Perret, J. Proriot, F. Prulhière
Laboratoire de Physique Corpusculaire, Université Blaise Pascal, IN²P³-CNRS, Clermont-Ferrand, 63177 Aubière, France
- J.D. Hansen, J.R. Hansen, P.H. Hansen, R. Møllerud, G. Petersen
Niels Bohr Institute, 2100 Copenhagen, Denmark¹²
- E. Simopoulou, A. Vayaki
Nuclear Research Center Demokritos (NRCD), Athens, Greece
- J. Badier, A. Blondel, G. Bonneaud, J. Bourotte, F. Braems, J.C. Brient, M.A. Ciocci, G. Fouque, R. Guirlet, A. Rougé, M. Rumpf, R. Tanaka, H. Videau, I. Videau¹
Laboratoire de Physique Nucléaire et des Hautes Energies, Ecole Polytechnique, IN²P³-CNRS, 91128 Palaiseau Cedex, France
- D.J. Candlin
Department of Physics, University of Edinburgh, Edinburgh EH9 3JZ, United Kingdom¹³
- A. Conti, G. Parrini
Dipartimento di Fisica, Università di Firenze, INFN Sezione di Firenze, 50125 Firenze, Italy
- M. Corden, C. Georgiopoulos, J.H. Goldman, M. Ikeda, J. Lannutti, D. Levinthal¹⁸, M. Mermikides, L. Sawyer, G. Stimpfl
Supercomputer Computations Research Institute and Dept. of Physics, Florida State University, Tallahassee FL 32306, USA^{15,16,17}
- A. Antonelli, R. Baldini, G. Bencivenni, G. Bologna⁶, F. Bossi, P. Campana, G. Capon, V. Chiarella, G. De Ninno, B. D'Ettorre-Piazzoli⁷, G. Felici, P. Laurelli, G. Mannocchi⁷, F. Murtas, G.P. Murtas, G. Nicoletti, P. Picchi⁶, P. Zografou
Laboratori Nazionali dell'INFN (LNF-INFN), 00044 Frascati, Italy
- B. Altoon, O. Boyle, A.W. Halley, I. ten Have, J.L. Hearn, J.G. Lynch, W.T. Morton, C. Raine, J.M. Scarr, K. Smith¹, A.S. Thompson
Department of Physics and Astronomy, University of Glasgow, Glasgow G12 8QQ, United Kingdom¹³

B. Brandl, O. Braun, R. Geiges, C. Geweniger¹, P. Hanke, V. Hepp, E.E. Kluge, Y. Maumary, M. Panter, A. Putzer, B. Rensch, A. Stahl, K. Tittel, M. Wunsch

Institut für Hochenergiephysik, Universität Heidelberg, 6900 Heidelberg, Fed. Rep. of Germany¹⁹

A.T. Belk, R. Beuselinck, D.M. Binnie, W. Cameron¹, M. Cattaneo, P.J. Dornan, S. Dugeay, R.W. Forty, A.M. Greene, J.F. Hassard, S.J. Patton, J.K. Sedgbeer, G. Taylor, I.R. Tomalin, A.G. Wright

Department of Physics, Imperial College, London SW7 2BZ, United Kingdom¹³

P. Girtler, D. Kuhn, G. Rudolph

Institut für Experimentalphysik, Universität Innsbruck, 6020 Innsbruck, Austria²¹

C.K. Bowdery¹, T.J. Brodbeck, A.J. Finch, F. Foster, G. Hughes, N.R. Keemer, M. Nuttall, B.S. Rowlingson, T. Sloan, S.W. Snow

Department of Physics, University of Lancaster, Lancaster LA1 4YB, United Kingdom¹³

T. Barczewski, L.A.T. Bauerdick, K. Kleinknecht¹, B. Renk, S. Roehn, H.-G. Sander, M. Schmelling, F. Steeg

Institut für Physik, Universität Mainz, 6500 Mainz, Fed. Rep. of Germany¹⁹

J-P. Albanese, J-J. Aubert, C. Bouchouk, A. Bonissent, D. Courvoisier, F. Etienne, E. Matsinos, S. Papalexioiu, P. Payre, B. Pietrzyk¹, Z. Qian

Centre de Physique des Particules, Faculté des Sciences de Luminy, IN²P³-CNRS, 13288 Marseille, France

W. Blum, P. Cattaneo, G. Cowan, B. Dehning, H. Dietl, M. Fernandez-Bosman, D. Hauff, A. Jahn, E. Lange, G. Lütjens, G. Lutz, W. Männer, H-G. Moser, Y. Pan, R. Richter, A.S. Schwarz, R. Settles, U. Stiegler, U. Stierlin, J. Thomas, G. Waltermann

Max-Planck-Institut für Physik und Astrophysik, Werner-Heisenberg-Institut für Physik, 8000 München, Fed. Rep. of Germany¹⁹

V. Bertin, G. de Bouard, J. Boucrot, O. Callot, X. Chen, A. Cordier, M. Davier, G. Ganis, J.-F. Grivaz, Ph. Heusse, P. Janot, V. Journé, D.W. Kim, J. Lefrançois, A.-M. Lutz, J.-J. Veillet, F. Zomer

Laboratoire de l'Accélérateur Linéaire, Université de Paris-Sud, IN²P³-CNRS, 91405 Orsay Cedex, France

S.R. Amendolia, G. Bagliesi, G. Batignani, L. Bosisio, U. Bottigli, C. Bradaschia, I. Ferrante, F. Fidecaro, L. Foà¹, E. Focardi, F. Forti, A. Giassi, M.A. Giorgi, F. Ligabue, A. Lusiani, E.B. Mannelli, P.S. Marrocchesi, A. Messineo, F. Palla, G. Sanguinetti, S. Scapellato, J. Steinberger, R. Tenchini, G. Tonelli, G. Triggiani

Dipartimento di Fisica dell'Università, INFN Sezione di Pisa, e Scuola Normale Superiore, 56010 Pisa, Italy

J.M. Carter, M.G. Green, P.V. March, T. Medcalf, M.R. Saich, J.A. Strong¹, R.M. Thomas, T. Wildish
Department of Physics, Royal Holloway & Bedford New College, University of London, Surrey TW20 OEX, United Kingdom¹³

D.R. Botterill, R.W. Clift, T.R. Edgecock, M. Edwards, S.M. Fisher, J. Harvey, T.J. Jones, P.R. Norton, D.P. Salmon, J.C. Thompson

Particle Physics Dept., Rutherford Appleton Laboratory, Chilton, Didcot, OXON OX11 0QX, United Kingdom¹³

B. Bloch-Devaux, P. Colas, C. Klopfenstein, E. Lançon, E. Locci, S. Loucatos, L. Mirabito, E. Monnier, P. Perez, F. Perrier, J. Rander, J.-F. Renardy, A. Roussarie, J.-P. Schuller

Département de Physique des Particules Élémentaires, CEN-Saclay, 91191 Gif-sur-Yvette Cedex, France²⁰

J.G. Ashman, C.N. Booth, F. Combley, M. Dinsdale, J. Martin, D. Parker, L.F. Thompson
Department of Physics, University of Sheffield, Sheffield S3 7RH, United Kingdom¹³

S. Brandt, H. Burkhardt, C. Grupen, H. Meinhard, E. Neugebauer, U. Schäfer, H. Seywerd
Fachbereich Physik, Universität Siegen, 5900 Siegen, Fed. Rep. of Germany¹⁹

B. Gobbo, F. Liello, E. Milotti, F. Ragusa⁸, L. Rolandi¹

Dipartimento di Fisica, Università di Trieste e INFN Sezione di Trieste, 34127 Trieste, Italy

L. Bellantoni, J.F. Boudreau, D. Cinabro, J.S. Conway, D.F. Cowen, Z. Feng, J.L. Harton, J. Hilgart, R.C. Jared⁹, R.P. Johnson, B.W. LeClaire, Y.B. Pan, T. Parker, J.R. Pater, Y. Saadi, V. Sharma, J.A. Wear, F.V. Weber, Sau Lan Wu, S.T. Xue, G. Zobernig

*Department of Physics, University of Wisconsin, Madison, WI 53706, USA*¹⁴

¹Now at CERN.

²Permanent address: DESY, Hamburg, Fed. Rep. of Germany.

³On leave of absence from SLAC, Stanford, CA 94309, USA.

⁴On leave of absence from University of Washington, Seattle, WA 98195, USA.

⁵Also Centre de Physique des Particules, Faculté des Sciences, Marseille, France

⁶Also Istituto di Fisica Generale, Università di Torino, Torino, Italy.

⁷Also Istituto di Cosmo-Geofisica del C.N.R., Torino, Italy.

⁸Now at INFN Milano.

⁹Permanent address: LBL, Berkeley, CA 94720, USA.

¹⁰Supported by CAICYT, Spain.

¹¹Supported by the National Science Foundation of China.

¹²Supported by the Danish Natural Science Research Council.

¹³Supported by the UK Science and Engineering Research Council.

¹⁴Supported by the US Department of Energy, contract DE-AC02-76ER00881.

¹⁵Supported by the US Department of Energy, contract DE-FG05-87ER40319.

¹⁶Supported by the NSF, contract PHY-8451274.

¹⁷Supported by the US Department of Energy, contract DE-FC05-85ER250000.

¹⁸Supported by SLOAN fellowship, contract BR 2703.

¹⁹Supported by the Bundesministerium für Forschung und Technologie, Fed. Rep. of Germany.

²⁰Supported by the Institut de Recherche Fondamentale du C.E.A..

²¹Supported by Fonds zur Förderung der wissenschaftlichen Forschung, Austria.

1. INTRODUCTION

The decay branching ratio of the Z^0 into a photon and a light pseudoscalar meson is predicted by the Standard Model to be unobservably small [1]. However it has been argued recently that such a decay could occur at a rate accessible to the LEP experiments [2, 3, 4]. Indeed, the branching ratio for the decay $Z^0 \rightarrow \pi^0 \gamma$ could be as large as 1.7×10^{-3} if the hypothesis of the Partially Conserved Axial Current (PCAC) still holds at LEP energies. Here a search for $Z^0 \rightarrow \pi^0 \gamma$ decays is reported. Given the difficulty of separating the two photons of a high-energy π^0 decay, such events would have the same topology as the QED process $e^+e^- \rightarrow \gamma\gamma$, namely two opposite electromagnetic clusters with almost the beam energy. Nonetheless, instead of falling as $1/s$, their rate would follow the resonant Z^0 line shape. Following the suggestion of Ref. [3], decays of the Z^0 into $\eta\gamma$ and $\eta'(958)\gamma$ are also searched for. In this case, the meson decay modes with two charged particles in the final state are more suitable, as the background expected from known processes is very low.

2. DESCRIPTION OF THE APPARATUS

A detailed description of the ALEPH detector is given in Ref. [5]. Here a brief description of the main components relevant to this analysis is given. These are the Inner Tracking Chamber (ITC), the Time Projection Chamber (TPC), the Electromagnetic Calorimeter (ECAL), and the Luminosity Calorimeter (LCAL).

The ITC is a set of eight concentric drift chamber layers. Tracks with $|\cos\theta| < 0.97$ cross all layers. The ITC is sensitive during the 250 ns after the beam crossing time. The TPC is placed inside a 1.5 T solenoidal superconducting magnet. It has 21 concentric circular pad rows which measure three-dimensional coordinates on charged tracks. Tracks at $|\cos\theta| < 0.95$ cross at least six pad rows.

The ECAL is a 22 radiation lengths sandwich of proportional tubes and lead plates. The signals collected on the tube wires provide a total energy trigger that is 100% efficient above 8 GeV. The calorimeter is hermetic down to angles of about 10° (i.e. $|\cos\theta| < 0.985$). It consists of three parts – one barrel and two end-caps – each of them separated in azimuth into twelve modules. The modules are finely segmented: cathode pads are grouped in projective towers pointing to the beam crossing point, covering an angular region of $1^\circ \times 1^\circ$ each. They are read out longitudinally in three stacks of 4, 9, and 9 radiation lengths. A finer longitudinal segmentation is provided by the readout of the 45 wire planes of each entire module separately, allowing an accurate analysis of isolated showers. The time of

arrival of the signal on the wire planes is also recorded, giving a measurement of the event time with an accuracy better than 50 ns for high-energy showers.

To make sure that the high voltage of the different parts of the apparatus is on, a special bit is set for each subdetector when the voltage reaches its nominal value, and this information is recorded with each event.

The integrated luminosity was measured by a lead-gas calorimeter covering the forward and backward region from 56 to 170 mrad around the beams. A total of $1.17 \pm 0.02 \text{ pb}^{-1}$, collected from the startup of the LEP collider until the end of December 1989, is used in this analysis.

3. SEARCH FOR $Z^0 \rightarrow \pi^0 \gamma$

3.1 EVENT SELECTION

The signature of this decay is two clusters in the ECAL, with no associated charged particle in the TPC. The TPC and the ECAL are required to be simultaneously operational, as is the LCAL for the measurement of the luminosity.

Events with no charged tracks are selected. However, to avoid a rejection due to false reconstruction in the ITC, where beam-related background can be high, events are also accepted if they have tracks that contain at most four hits in the TPC and have a momentum smaller than 500 MeV/c. One event is observed in this category. Photon conversions can give rise to tracks of higher momentum and cause an inefficiency which is estimated from Monte Carlo simulations of $\gamma\gamma$ annihilation events to be $10.7 \pm 1.0\%$.

An energy deposit above 20 GeV is required on the wire planes of at least two modules of the ECAL. Furthermore, events are only selected if the two most energetic clusters have a polar angle in the range $|\cos \theta| < 0.95$. To reject cosmic showers spanning two modules, the angle in space between the two clusters is required to be greater than 120° . These conditions are met by 75 events. By scanning this sample, events are found where no tracks with more than four hits in the TPC were reconstructed, but where two tracks or two sets of points exist, which are aligned with the ECAL clusters. There are 28 such poorly reconstructed low-angle events, which are removed from the data sample. They pass the selection criteria because of dead regions between the TPC sectors and small pattern recognition inefficiencies. From Monte Carlo simulation, 24.5 ± 4.2 such events are expected, arising from about 2700 Bhabha events whose ECAL clusters satisfy the above criteria. This leaves a sample of 47 unambiguous photon-pair candidates. The lateral and

longitudinal profiles of the clusters are found to be compatible with the expected shape of electromagnetic showers.

Two features allow to distinguish between $\gamma\gamma$ and any remaining e^+e^- events, namely:

- i) The electromagnetic shower from a photon is expected to start later in the calorimeter than that from an electron.
- ii) The electron tracks are bent by the magnetic field, which causes an apparent misalignment of the two showers with the interaction point in the plane transverse to the beam. Initial-state bremsstrahlung effects are minimal in this plane.

The comparison of the average longitudinal profile between $e^+e^- \rightarrow e^+e^-$ events and the $\gamma\gamma$ sample (see Fig. 1) shows a clear shift of about one radiation length, in agreement with the expectation for photons.

In Fig. 2, the distribution of $\Delta\phi$, the angle between the projections of the two most energetic clusters onto the plane transverse to the beam is shown, both for the selected events and for $e^+e^- \rightarrow e^+e^-$ data. It is seen that the events from the $\gamma\gamma$ sample are peaked at 180° whereas the $e^+e^- \rightarrow e^+e^-$ events are peaked at 178° because of the bending in the magnetic field. This shows that the event sample is not contaminated by $e^+e^- \rightarrow e^+e^-$ events with charged tracks lost in the readout chain.

Data were taken at eight different points in energy, going from -3 GeV to $+4$ GeV around the Z^0 peak (91.3 GeV) in steps of 1 GeV. The number of events left after the selection as a function of \sqrt{s} is presented in Table 1.

3.2 COMPARISON WITH EXPECTATIONS FROM QED

In order to take into account the acceptance of the apparatus and the conversion of photons in matter, Monte Carlo events are generated according to QED predictions and propagated through the apparatus. These simulated events are then processed through the normal reconstruction and analysis chain.

For the event generation, the Monte Carlo program of Berends and Kleiss [6] is used, which produces two- and three-photon final states. The first-order radiative corrections are taken into account; they result in an 11% increase of the cross-section with respect to the Born contribution. The total production cross-section of photon pairs is predicted to be 47.0 pb at 91.3 GeV centre-of-mass energy for $|\cos\theta| < 0.95$. The simulation uses the ALEPH Monte Carlo program, which contains a description of the materials of the detector; it takes into account the detailed geometry and readout, and produces simulated

raw data in the same format as the actual detector. A detection and selection efficiency of $80.7 \pm 1.3\%$ is found by this procedure. This includes the aforementioned loss due to photon conversions.

The distributions of the total energy and the cosine of the polar angle of the two highest-energy clusters are shown in Fig. 3, and are compared with the QED Monte Carlo prediction. The angle with the beam direction is calculated in the centre of mass of the two-photon system.

The expected number of events at each centre-of-mass energy is given in Table 1. The agreement of the data with QED predictions is good, and this allows to derive a limit on the partial decay width of the Z^0 into $\pi^0\gamma$.

3.3 LIMIT ON THE PARTIAL DECAY WIDTH FOR $Z^0 \rightarrow \pi^0\gamma$

To estimate the efficiency of selecting the $Z^0 \rightarrow \pi^0\gamma$ decays, such events were generated according to the expected angular distribution [3, 4]

$$\frac{dN}{d\cos\theta} \propto 1 + \cos^2\theta$$

and propagated through the detector and analysis chain as was done for the QED background. This takes into account higher losses than in the QED case ($13.2 \pm 1.7\%$ instead of $10.7 \pm 1.0\%$), due to a higher number of photon conversions, since there are generally three photons instead of two in these events. The overall efficiency $\epsilon_{\pi^0\gamma}$ is found to be $72.6 \pm 2.0\%$ (92.7% from the $\cos\theta$ cut and 78.3% from the detection and selection; this includes the effects of photon conversions and losses in the cracks of the calorimeter).

The expected numbers of $\pi^0\gamma$ events (in addition to the QED background) for a branching fraction of 1.7×10^{-3} are shown in the last column of Table 1. It is seen that most of the sensitivity is concentrated near the peak (91.3 GeV), where both the cross-section and the recorded luminosity are large. To calculate the upper limit, the likelihood function is defined to be the product of the Poisson probabilities for observing n_i^{obs} events at the centre-of-mass energy E_i , when expecting n_i^{exp} events

$$n_i^{exp} = n_i^{\gamma\gamma} + n_i^{\pi^0\gamma}(B_{Z^0 \rightarrow \pi^0\gamma}),$$

i.e. it is a function of the unknown branching ratio $B_{Z^0 \rightarrow \pi^0\gamma}$. The numbers are given in Table 1: for each energy E_i (col. 1) there are n_i^{obs} observed events (col. 5), $n_i^{\gamma\gamma}$ events

expected from QED $\gamma\gamma$ production (col. 4), and $n_i^{\pi^0\gamma}(B_{Z^0\rightarrow\pi^0\gamma})$ events of the $\pi^0\gamma$ final state. This last number is simply the product of the total number of Z^0 's by $B_{Z^0\rightarrow\pi^0\gamma}$ and the efficiency $\epsilon_{\pi^0\gamma}$. The 95% confidence level (C.L.) limit is the value of $B_{Z^0\rightarrow\pi^0\gamma}$ such that the area under the normalized likelihood curve between 0 and $B_{Z^0\rightarrow\pi^0\gamma}$ is 0.95. This leads to a limit of 4.9×10^{-4} on the branching ratio. The corresponding 99% C.L. limit is 6.8×10^{-4} . These limits depend on the values of the luminosity and the efficiencies $\epsilon_{\gamma\gamma}$ and $\epsilon_{\pi^0\gamma}$. Their errors are taken into account by increasing or reducing these values by one standard deviation in order to make the limits more conservative. This increases the limits by about 10%. Using the measured total width of the Z^0 from Ref. [7] of $\Gamma_{tot} = 2.541 \pm 0.056$ GeV, this limit corresponds to a $Z^0 \rightarrow \pi^0\gamma$ partial width $\Gamma_{Z^0\rightarrow\pi^0\gamma} < 1.3$ MeV. At 99% C.L., an upper limit of $\Gamma_{Z^0\rightarrow\pi^0\gamma} < 1.8$ MeV is found.

4. SEARCH FOR $Z^0 \rightarrow \eta\gamma$ AND $Z^0 \rightarrow \eta'\gamma$

4.1 EVENT SELECTION

In the search for decays of the Z^0 into $\eta\gamma$ and $\eta'\gamma$, those decay modes of the mesons that result in two oppositely-charged particles in addition to any number of photons and π^0 's are used. The total branching fraction for such decays of the η is $29.1 \pm 0.5\%$, while it is $70.1 \pm 1.9\%$ for the η' [8]. Hence only those events are selected that contain exactly two oppositely-charged tracks, each having at least four well-measured coordinates in the TPC. The invariant mass of these two tracks is required to be less than 1 GeV, where the particles are assigned the charged-pion mass and their momenta are evaluated at the point of closest approach to the beam-crossing point. There are 756 such two-track events. In addition, it is required that the energy of this charged-particle pair, as measured in the TPC, be greater than 10 GeV, and that the angle between the vector sum of the two track momenta and the beam direction be greater than 30° and less than 150° . This condition rejects background from two-photon collisions and beam-gas events. Note that the event selection uses only information from the tracking detectors. The above selection criteria lead to one candidate event, which has the two charged particles associated with a cluster of 45.0 GeV in the ECAL, with an isolated cluster of 42.3 GeV on the opposite side of the ECAL. The charged particles in this event have momenta of 32.4 GeV and 6.0 GeV and are consistent with being an e^+e^- pair from photon conversion in the material at the boundary between the ITC and the TPC, as determined by a pair-finding algorithm. There are no hits in the ITC belonging to these two tracks. Furthermore, the energy of the pair as measured from the tracks is consistent with the energy deposited in the cluster with

which they are associated. Hence one can classify this event as a $\gamma\gamma$ final state, where one of the photons underwent pair conversion in the detector material. This event occurred at a centre-of-mass energy of 88.3 GeV. After removing this event there are thus no observed candidates.

4.2 LIMIT ON THE PARTIAL DECAY WIDTHS FOR $Z^0 \rightarrow \eta\gamma$ AND $Z^0 \rightarrow \eta'\gamma$

Since there are no observed events, upper limits at 95% C.L. on the branching ratios for $Z^0 \rightarrow \eta\gamma$ and $Z^0 \rightarrow \eta'\gamma$ can be derived. They are given by those values for $B_{Z^0 \rightarrow \eta\gamma}$ and $B_{Z^0 \rightarrow \eta'\gamma}$ for which it is expected to observe $N_{exp} = 3$ events. Here N_{exp} is the number of events expected, taking into account the line shape of the Z^0 resonance as measured in this experiment [7]. The total number of Z^0 's produced in the whole beam energy range, including invisible decays, is estimated to be 35525.

From Monte Carlo simulations of the final states $\eta\gamma$ and $\eta'\gamma$, the efficiencies of the event selection cuts are determined to be $\epsilon_{\eta\gamma} = 69.1 \pm 6.3\%$ and $\epsilon_{\eta'\gamma} = 58.8 \pm 3.9\%$ for the decay channels with two charged particles. As more than half of the total energy in these final states is electromagnetic, the trigger is fully efficient.

These numbers translate into limits on the branching ratios of $B_{Z^0 \rightarrow \eta\gamma} < 4.6 \times 10^{-4}$ and $B_{Z^0 \rightarrow \eta'\gamma} < 2.2 \times 10^{-4}$. Using the measured total width of the Z^0 , limits are obtained for the partial decay widths of the Z^0 of $\Gamma_{Z^0 \rightarrow \eta\gamma} < 1.2$ MeV and $\Gamma_{Z^0 \rightarrow \eta'\gamma} < 0.6$ MeV at 95% C.L.

5. CONCLUSION

The decays of the Z^0 into a pseudoscalar meson and a photon have been searched for and no evidence has been found for resonant production of a photon and a meson (π^0 , η , η') at the Z^0 peak.

The study of the $Z^0 \rightarrow \pi^0\gamma$ channel was performed by selecting events with at least two high-energy electromagnetic clusters. The agreement of the rate for these events with QED predictions allowed to give a limit on the branching ratio $B_{Z^0 \rightarrow \pi^0\gamma} < 4.9 \times 10^{-4}$, at 95% C.L., corresponding to a limit on the partial width $\Gamma_{Z^0 \rightarrow \pi^0\gamma} < 1.3$ MeV.

For the $Z^0 \rightarrow \eta\gamma$ and $Z^0 \rightarrow \eta'\gamma$ channels, the charged decay modes have been used to set the following 95% C.L. limits : $B_{Z^0 \rightarrow \eta\gamma} < 4.6 \times 10^{-4}$ and $B_{Z^0 \rightarrow \eta'\gamma} < 2.2 \times 10^{-4}$, corresponding to $\Gamma_{Z^0 \rightarrow \eta\gamma} < 1.2$ MeV and $\Gamma_{Z^0 \rightarrow \eta'\gamma} < 0.6$ MeV.

Acknowledgements

We would like to thank our colleagues of the LEP Division for their outstanding performance in bringing the LEP machine into operation. We thank also the engineers and technicians in all our institutions for their support in constructing ALEPH. Those of us from non-member countries wish to thank CERN for its hospitality.

REFERENCES

1. L. Arnellos, W.J. Marciano and Z. Parsa, Nucl. Phys. **B196** (1982) 378.
2. C.-H. Chang, Y.-Q. Chen, Y.-P. Kuang, J.-X. Wang and D.-D. Wu, "A calculation on $Z^0 \rightarrow \pi^0 \gamma$ decay with PCAC and the triangle anomaly", Beijing preprint AS-ITP-88-049.
3. M. Jacob and T.T Wu, Phys. Lett. **B232** (1989) 529.
4. S. Ghosh and D. Chatterjee, "Anomaly induced Z-boson interactions", Saha Institute of Nuclear Physics preprint, Calcutta, SINP/TNP /89-24 (1989).
5. D. Decamp et al. (ALEPH Collab.), "ALEPH: A detector for electron-positron annihilations at LEP", preprint CERN-EP/90-25, submitted to Nucl. Instrum. Methods (1990).
6. F.A. Berends, R. Kleiss, P. de Causmaecker, R. Gastmans and W. Troost, Nucl. Phys. **B206** (1982) 61.
7. D. Decamp et al. (ALEPH Collab.), "A precise determination of the number of families with light neutrinos and of the Z boson partial widths", preprint CERN-EP/89-169 (1989), submitted to Phys. Lett. B.
8. Review of Particle Properties, Phys. Lett. **B204** (1988).

Table 1. For each centre-of-mass energy point around the peak (91.3 GeV), are listed: the total number of Z^0 's produced (including neutrino decay modes), the recorded luminosity, the number of photon pairs expected within the acceptance, the number of photon pairs observed, and the number of additional events expected from the $Z^0 \rightarrow \pi^0\gamma$ process for a branching ratio of 1.7×10^{-3} . About half of the data were taken on the Z^0 peak.

c.m. energy	No. of Z^0 's	Luminosity (nb ⁻¹)	$N_{\gamma\gamma}^{\text{exp}}$	$N_{\gamma\gamma}^{\text{obs}}$	$N_{\pi^0\gamma}^{\text{exp}}$ (BR = 1.7×10^{-3})
-3 GeV	746.7	111.8	4.5	6	0.9
-2 GeV	806.6	63.6	2.5	1	1.0
-1 GeV	3320.7	120.8	4.7	6	4.1
Peak	24256.2	563.8	21.4	16	29.9
+1 GeV	3982.0	136.7	5.1	4	4.9
+2 GeV	1458.2	86.1	3.1	9	1.8
+3 GeV	816.3	74.1	2.6	3	1.0
+4 GeV	138.5	16.2	0.6	2	0.2
TOTAL	35525 ± 783	1173 ± 20	44.5 ± 1.1	47	43.8 ± 1.4

Figure captions

- Fig. 1 Longitudinal profile of electromagnetic showers, both for electrons from $e^+e^- \rightarrow e^+e^-$ and for the $\gamma\gamma$ candidates. Both samples are real data. There is a clear shift by about 1 radiation length of the photon showers with respect to electron showers, as expected.
- Fig. 2 Angle between the projections of the two centroids of the clusters, for $\gamma\gamma$ candidates (hatched histogram, one event is off-scale to the left), and $e^+e^- \rightarrow e^+e^-$ events (normalized to the same area). The effect of the curvature of the electron trajectories in the magnetic field is clearly visible.
- Fig. 3 Kinematical distributions from the $\gamma\gamma$ sample, compared to the QED Monte Carlo simulation. a) Sum of the energies of the two clusters divided by the centre-of-mass energy; b) cosine of the polar angle of the two-photon system in its rest frame.

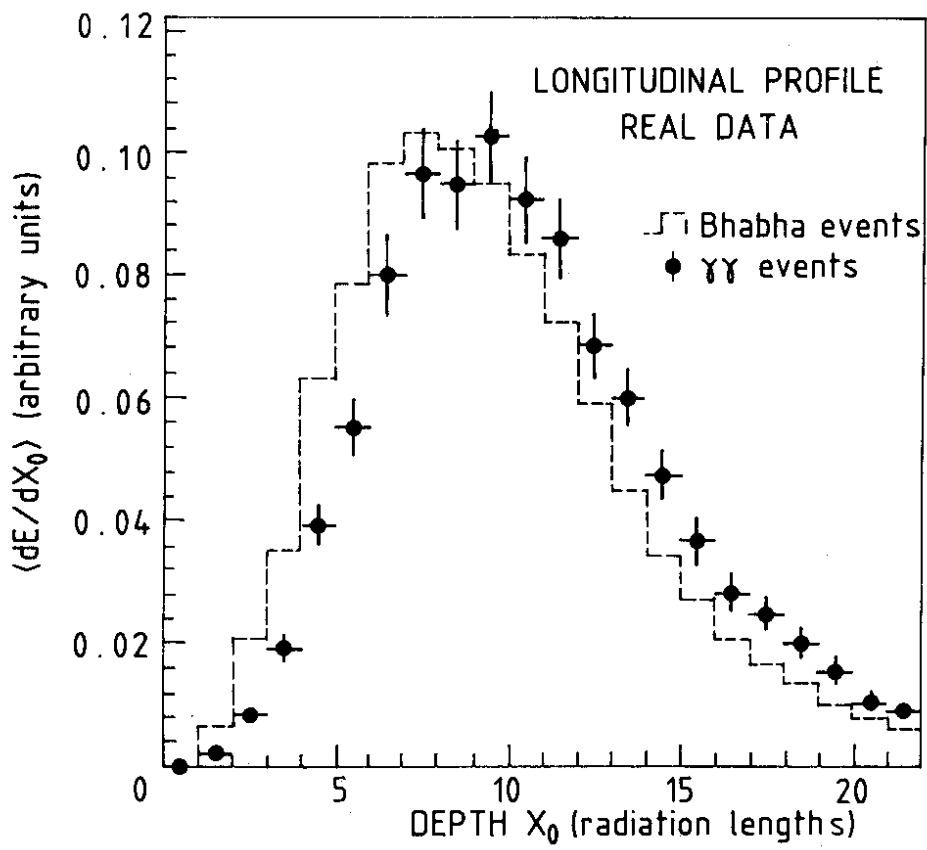


Fig. 1

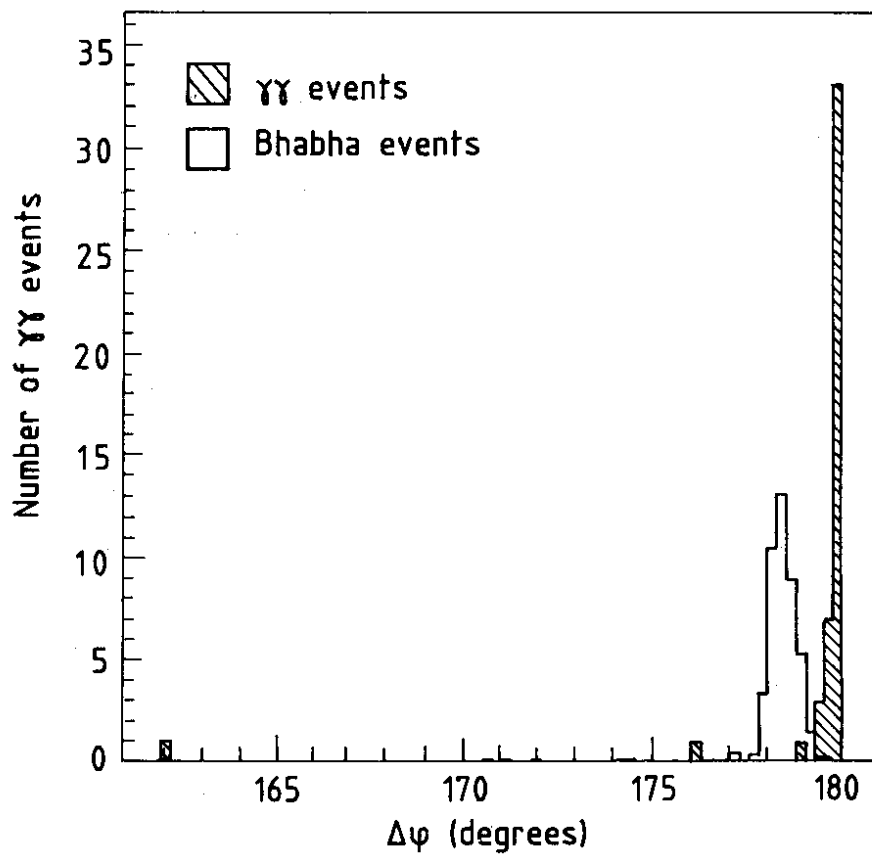


Fig. 2

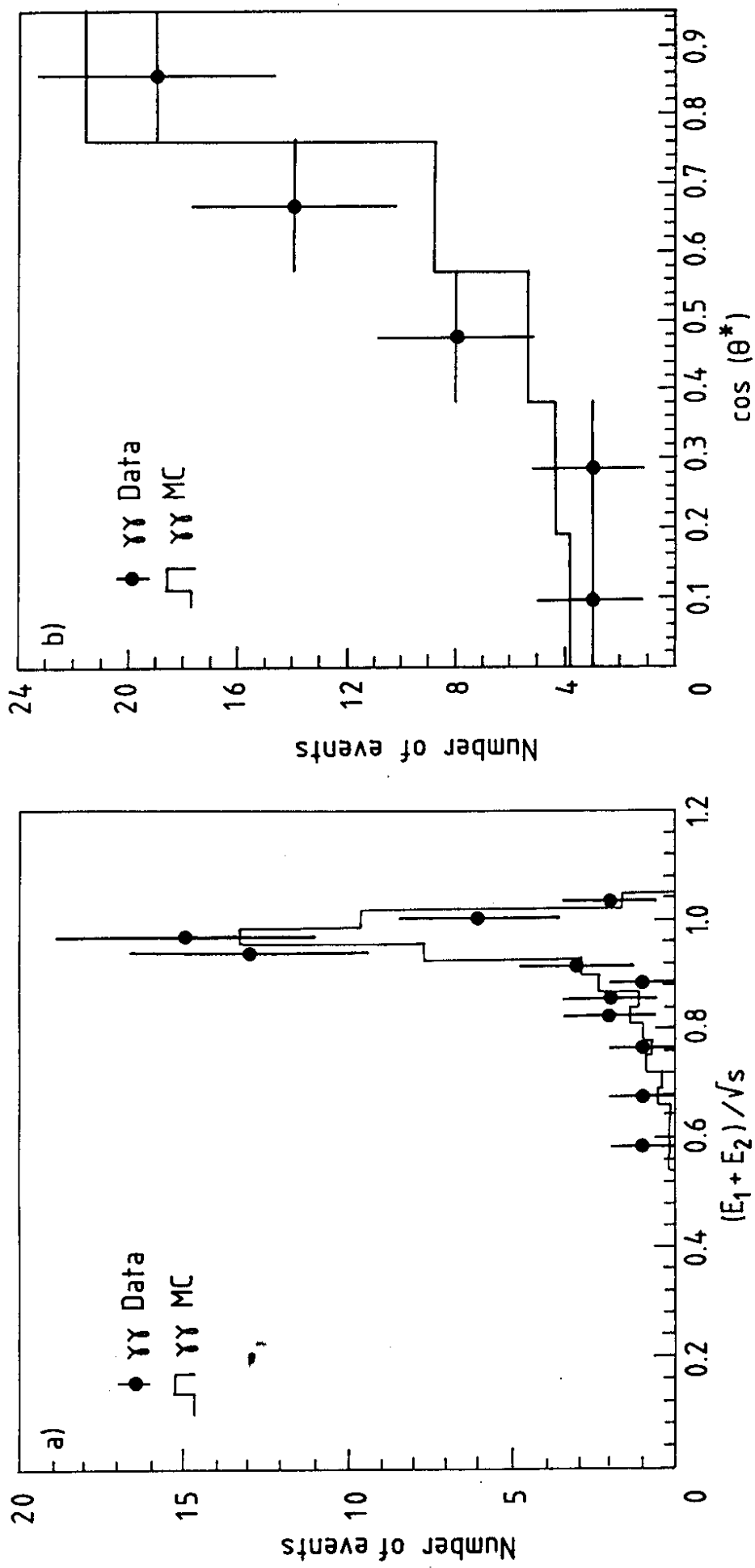


Fig. 3